

Geophysical Research Letters®

RESEARCH LETTER

10.1029/2021GL095751

Key Points:

- During the recovery phase of a small geomagnetic storm, substorm activity drove a new set of FACs into the ionosphere, initiating a sub-auroral polarization stream (SAPS)
- The SAPS location remained relatively constant, firmly inside the trough, independent of the variability in the field-aligned currents (FACs)
- The SAPS flows were sustained for almost an hour after the FACs weakened and retreated polewards

Supporting Information:

Supporting Information may be found in the online version of this article.

Correspondence to:

B. S. R. Kunduri,
bharatr@vt.edu









Citation:

Kunduri, B. S. R., Baker, J. B. H., Ruohoniemi, J. M., Coster, A. J., Vines, S. K., Anderson, B. J., et al. (2021). An examination of magnetosphere-ionosphere influences during a SAPS event. *Geophysical Research Letters*, 48, e2021GL095751. <https://doi.org/10.1029/2021GL095751>

Received 17 AUG 2021

Accepted 20 SEP 2021

An Examination of Magnetosphere-Ionosphere Influences During a SAPS Event

B. S. R. Kunduri¹ , J. B. H. Baker¹ , J. M. Ruohoniemi¹ , A. J. Coster² , S. K. Vines³ ,
B. J. Anderson³ , S. G. Shepherd⁴ , and A. T. Chartier³ 

¹Bradley Department of Electrical and Computer Engineering, Virginia Tech, Blacksburg, VA, USA, ²MIT Haystack observatory, Westford, MA, USA, ³The Johns Hopkins University Applied Physics Laboratory, Laurel, MD, USA,

⁴Thayer School of Engineering, Dartmouth College, Hanover, NH, USA

Abstract The sub-auroral polarization stream (SAPS) is a region of westward high velocity plasma convection equatorward of the auroral oval that plays an important role in mid-latitude space weather dynamics. In this study, we present observations of SAPS flows extending across the North American sector observed during the recovery phase of a minor geomagnetic storm. A resurgence in substorm activity drove a new set of field-aligned currents (FACs) into the ionosphere, initiating the SAPS. An upward FAC system is the most prominent feature spreading across most SAPS local times, except near dusk, where a downward current system is pronounced. The location of SAPS flows remained relatively constant, firmly inside the trough, independent of the variability in the location and intensity of the FACs. The SAPS flows were sustained even after the FACs weakened and retreated polewards with a decline in geomagnetic activity. The observations indicate that the mid-latitude trough plays a crucial role in determining the location of the SAPS and that SAPS flows can be sustained even after the magnetospheric driver has weakened.

Plain Language Summary The sub-auroral polarization stream (SAPS) is an important phenomenon that controls the dynamics of the sub-auroral region. While SAPS has been studied for several decades, our understanding of the drivers of this phenomenon is still limited. In this study, we analyze an event to examine the validity of different SAPS mechanisms, and to determine the importance of the ionosphere-thermosphere system in driving and sustaining SAPS flows. We find that the ionosphere can play an important role in determining SAPS location and that SAPS can be sustained even after the magnetospheric driver has weakened.

1. Introduction

Sub-auroral polarization stream (SAPS) is a prominent large-scale manifestation of sub-auroral magnetosphere-ionosphere (MI) coupling and plays an important role in controlling and driving inner magnetosphere-ionosphere dynamics (Erickson et al., 2011; Ferdousi et al., 2019; Kunduri et al., 2017; Lejosne et al., 2018). Over the last few decades, different mechanisms have been proposed to explain SAPS observations under different geomagnetic conditions. The early theory of SAPS generation suggested that during periods of enhanced geomagnetic activity, a misalignment between the ion and electron Alfvén layers (Gussenhoven et al., 1987; Heinemann et al., 1989) generates strong poleward-directed electric fields (P. C. Anderson et al., 1993, 2001) that drive westward $E \times B$ drifts. Later, P. C. Anderson et al. (1993) proposed that the precipitation boundary misalignment also causes a portion of the Region-2 field-aligned currents (FACs) to flow into a region of low conductance, called the mid-latitude trough. As a result, current closure between Region-2 and Region-1 currents is inhibited leading to the generation of the large poleward directed SAPS electric fields (P. C. Anderson et al., 1993; He et al., 2018). It has been suggested that Joule heating produced by these strong SAPS electric fields can increase the ion recombination rate, resulting in a further decrease in conductivity (Banks & Yasuhara, 1978; Schunk et al., 1976). This produces an ionosphere-thermosphere feedback effect that allows the electric fields to grow even more (P. C. Anderson et al., 1993, 2001) which in turn further decreases the conductivity, and so on.

More recently, increased observational coverage in the sub-auroral ionosphere and the inner magnetospheric region have provided new insights into the SAPS phenomenon, and alternative theories have been pro-

posed (e.g., Mishin et al., 2017; Sangha et al., 2020). In particular, several studies have examined the association of SAPS with substorm activity (Mishin, 2016; Mishin et al., 2017; Parkinson et al., 2003). Specifically, it has been suggested that the substorm current wedge (SCW) is made up of not one but two pairs of FACs (Birn & Hesse, 2013; Kepko et al., 2015; Murphy et al., 2013), with one pair flowing into/out of the ionosphere in the dawn/dusk sector on the poleward edge (the outer loop) and another pair with the opposite sense on the equatorward edge (the inner loop). These two pairs of FACs have been referred to as the “two-loop substorm current wedge” in recent literature (Kepko et al., 2015), and some studies (Mishin, 2016; Mishin et al., 2017) have proposed that current closure in the two-loop substorm current wedge can also drive westward flows similar to storm-time SAPS.

In this study, we present Super Dual Auroral Radar Network (SuperDARN) observations of westward directed SAPS flows from July 5, 2011, during the recovery phase of a minor geomagnetic storm. We compare with AMPERE FACs and GPS TEC data to show that the location of SAPS flows is strongly dependent on the thermosphere-ionosphere processes can play an important role in specifying SAPS latitude and sustaining the flows even after the magnetospheric driver has weakened.

2. Data Sets

SuperDARN is an international network of HF radars covering polar, high and middle latitudes in the northern and southern hemispheres. Over the past several decades, measurements provided by SuperDARN have played an important role in advancing our knowledge of ionospheric electrodynamics (Chisham et al., 2007; Nishitani et al., 2019). In brief, SuperDARN radars make measurements of coherent backscatter from decameter-scale magnetic field aligned plasma irregularities and the Doppler shift of the backscattered signal is proportional to the line-of-sight component of the $\mathbf{E} \times \mathbf{B}$ plasma drift in the scattering region (Ruohoniemi et al., 1987). The radars electronically steer their look directions, typically scanning through 24 beams in 1 min and covering an azimuth of $\sim 50^\circ$. In this study, we use Line-of-Sight velocities (V_{LOS}) of ionospheric plasma flows, as well as L-shell fitted SAPS velocity vectors (Kunduri et al., 2018) from five U.S mid-latitude radars (WAL, FHE, FHW, CVE, and CVW) to analyze SAPS flows during an event that took place on July 5, 2011.

Hemispheric maps of the FACs are provided by the Active Magnetosphere and Planetary Electrodynamics Response Experiment (AMPERE) project (B. J. Anderson et al., 2000), using measurements from the magnetometers on board the Iridium® satellite constellation (B. J. Anderson et al., 2000; Waters et al., 2001). The Iridium constellation comprises 60+ commercial satellites in 780 km polar circular orbits, distributed over six equally spaced orbital planes, with 2 hr local time separation. Perturbations measured by magnetometers on-board each satellite are ingested by a spherical harmonic inversion technique to derive the hemispheric configuration of FACs in the polar regions (Waters et al., 2001). These FAC maps are provided at 10 min cadence with spatial resolution of 1-hr in magnetic local time (MLT) and 1° in magnetic latitude (MLAT).

Global Positioning System (GPS) Total Electron Content (TEC) measurements provided by the Madrigal database are used to analyze the location and depth of the ionospheric mid-latitude trough. The TEC data are processed using the algorithms described in Rideout and Coster (2006); Vierinen et al. (2016) and are binned into $1^\circ \times 1^\circ$ cells with an update every 5 min. In this study, the median filtering technique described in Thomas et al. (2013) is used to process the global GPS TEC maps for improving the spatial coverage provided by the distributed receivers. We identify the mid-latitude trough as the region between 50° – 65° MLAT where TEC values were lower than 8 TECU. These values were selected by visual inspection.

3. Observations

The main goal of this study is to examine the location and dynamics of the SAPS flows in relation to the configuration of FACs and the ionospheric trough. We begin with an overview of the background geomagnetic conditions during the event interval. In Figure 1, we present a time series spanning July 4–5, 2011, of (from top to bottom): IMF Bz from the OMNI data set (King & Papitashvili, 2005), AL/AU indices (Davis & Sugiura, 1966) and SYM-H/ASY-H indices (Iyemori, 1990). The green highlighted region identifies the interval between 0300 and 0700 UT on July 5, 2011 when SAPS flows were observed by mid-latitude SuperDARN

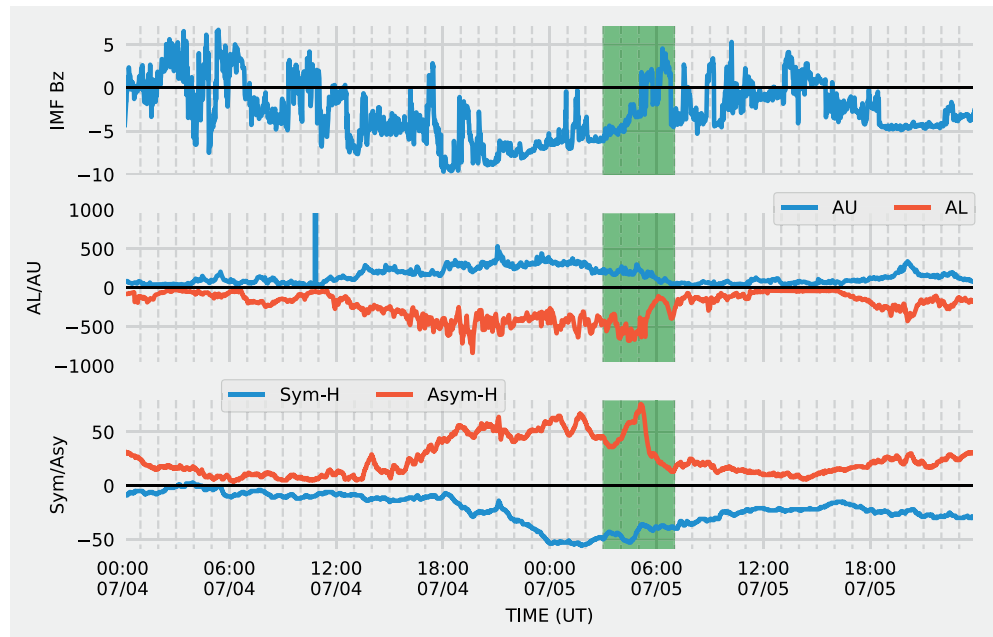


Figure 1. Interplanetary and geomagnetic activity on July 4–5, 2011. From top to bottom: IMF Bz, AU/AL indices and SYM-H/ASY-H indices. The green shaded region identifies the time interval of interest between 0300 and 0700 UT on July 5, 2011 when a resurgence in substorm activity occurred and sub-auroral polarization stream flows developed.

radars. This interval is characterized by weakening southward IMF and increasing SYM-H index (min value ~ -50 nT), consistent with the recovery phase of a minor storm. Elevated AL magnitude (~ -650 nT) and an uptick in ASY-H (max value ~ 70 nT) are indicative of ongoing substorm activity and enhancement of the partial ring current, both considered favorable for the development of SAPS (P. C. Anderson et al., 1993; Makarevich et al., 2011).

In Figure 2, we show the evolution of the SAPS event using snapshots of SuperDARN, AMPERE and GPS TEC observations at different time instances. Specifically, we present observations at 0400, 0420, and 0500 UT to show the formation and intensification of the SAPS, and 0545, 0615, and 0635 UT to show the declining phase of the SAPS. Line-of-sight velocities (V_{LOS}) measured by five US mid-latitude SuperDARN (WAL, FHE, FHW, CVE, and CVW) radars and AMPERE FAC observations are shown in the left panels, while median filtered GPS TEC measurements and SuperDARN V_{LOS} are shown in the right panels. The maps are shown in the new version of the Altitude-Adjusted Corrected Geomagnetic (AACGM) coordinates (Shepherd, 2014). Note that the westward/eastward oriented radars are measuring negative/positive V_{LOS} indicating that the flows are predominantly westward. SAPS speeds were found to vary between 200 and 1200 m/s during this event. The MLAT of the flows was compared with particle precipitation measurements from nearby POES satellite passes to confirm that they are located equatorward of the auroral oval (not shown). The left panels show SAPS flows first formed near dusk but subsequently expanded across mid-night to form a well-defined MLT-extended structure firmly embedded within a similarly MLT-extended TEC trough. By contrast, the FACs are much more variable with MLT and categorizing them into distinct Region-1, Region-2, and Substorm Current Wedge (SCW) features is difficult on the night side. The declining phase of the event is characterized by a poleward retreat of the FACs that is highly asymmetric with MLT, being faster at midnight and slower toward dusk. In contrast, the SAPS flows weaken in place as the FACs retreat and persist much longer at midnight, firmly embedded in the TEC trough, which has a similarly stable MLAT-MLT structure. Overall, the trough seems to play an important role in setting SAPS MLAT and sustaining the flows even after the FACs have retreated poleward and weakened.

We now further examine the location of the SAPS flows in relation to the FACs and the TEC trough. Figure 3 shows MLAT versus time keograms of median filtered FAC densities (left panels) and GPS TEC measurements (right panels) with overlaid dots showing the location of SuperDARN observed SAPS flows. In this

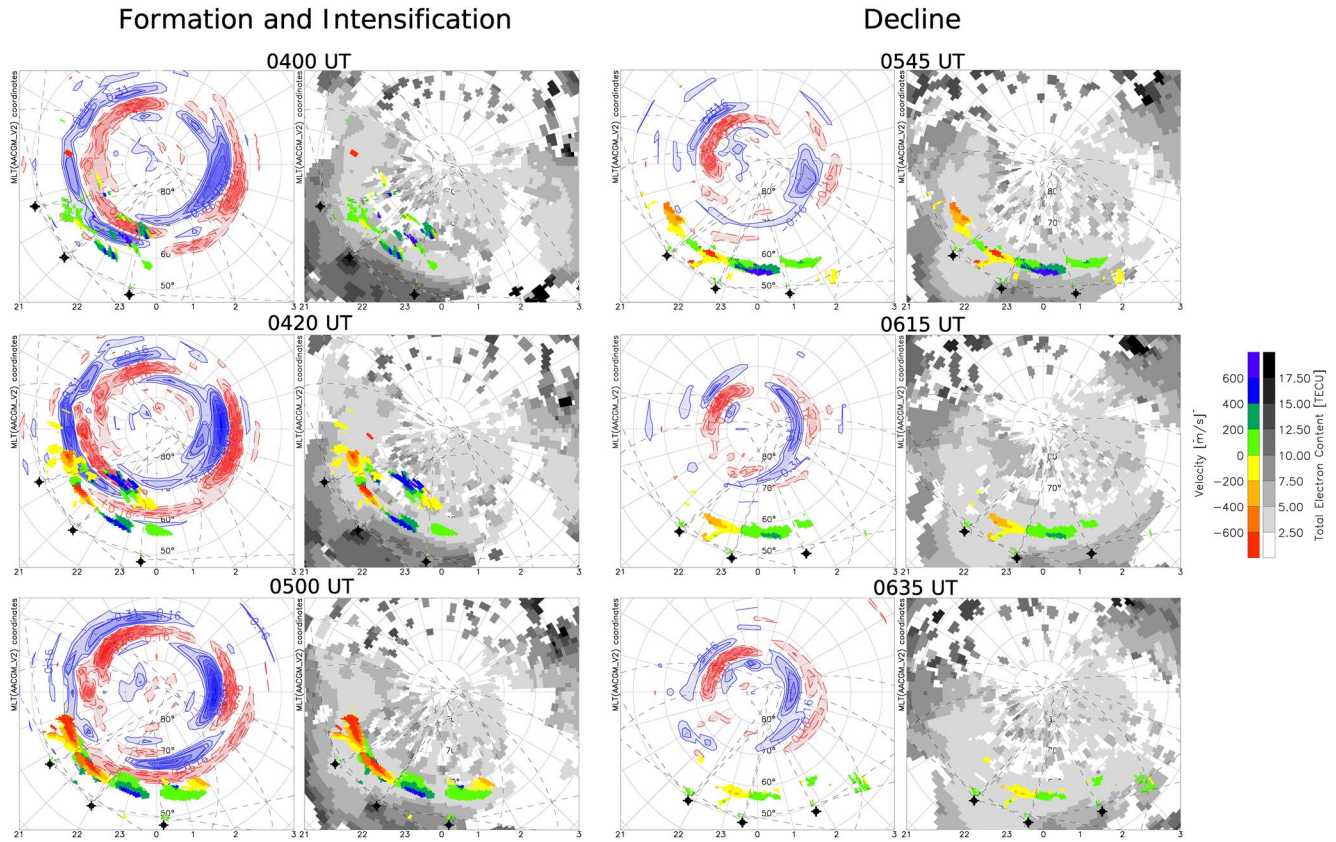


Figure 2. Observations of Super Dual Auroral Radar Network (SuperDARN) plasma flows, Active Magnetosphere and Planetary Electrodynamics Response Experiment field-aligned currents (AMPERE FACs), and Global Positioning System total electron content (GPS TEC) measurements on July 5, 2011 at select times from 0400 to 0635 UT. At each time instance, the left panel shows field-aligned currents from the AMPERE data set and the line-of-sight velocities measured by five US mid-latitude SuperDARN radars, and the right panels show median filtered GPS TEC observations overlaid with SuperDARN line-of-sight velocities. Fields-of-view of the contributing SuperDARN radars are also overlaid on all panels.

study, V_{LOS} from the five mid-latitude SuperDARN radars which were located below the equatorward edge of the auroral oval (estimated using measurements from POES satellites; see (Kunduri et al., 2017) for a detailed description of the methodology) and directed westwards were classified as belonging to SAPS. These V_{LOS} from SAPS were then resolved into 2-D velocity vectors by using a L-shell fitting method described in (Kunduri et al., 2018). The panels correspond to 19, 22, and 0 MLT. For this time-series correlation analysis, we apply a simple spatio-temporal median filtering technique to remove small-scale FAC features that are transitory and/or have a local-time extent narrower than what can be confidently resolved in the AMPERE data set considering the separation of the Iridium orbital planes. Specifically, for a given location and time instance, we discard any features that persist for less than 20 min over a 40 min interval, and less than 2 out of the 4 surrounding hours of MLT. The left panels show most of the SAPS flows near 19 MLT (upper panel) are located equatorward of a downward current region while those at 22 and 0 MLT are mostly equatorward of an upward current region. None of the SAPS flows form in a region between pronounced upward and downward currents. At all MLTs, the SAPS flows stay relatively fixed in MLAT as the FACs retreat poleward and decay in strength. At 0 MLT, the SAPS flows persist for more than an hour after the upward FAC has essentially disappeared. The right panels show that the latitude of the SAPS flows closely track the TEC trough MLAT. Overall, the location of the SAPS flows seems to have a stronger relationship to the trough than to the FACs, at least during this interval. Figure 4 shows time-series plots of SAPS speed compared with the median values of the upward current strength (J_{SCW}^{\uparrow}) shown in the upper panels and the depth of the TEC trough shown in the lower panels, at 22 MLT (left) and 0 MLT (right). The upper panels show that the SAPS speed tracks the magnitude of the upward current quite well at 22 MLT (0.7 correlation) but not at 0 MLT (−0.4 correlation). Field-aligned current closure is thus a plausible driver of the SAPS flows

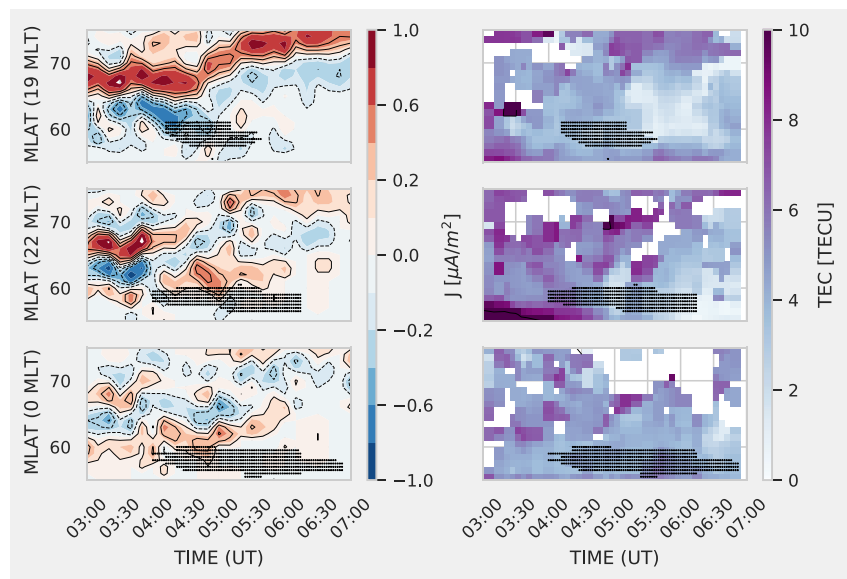


Figure 3. Magnetic latitude (MLAT) versus UT Keograms showing sub-auroral polarization stream (SAPS) latitude compared with Active Magnetosphere and Planetary Electrodynamics Response Experiment field-aligned current (AMPERE FAC) densities and Global Positioning System total electron content (GPS TEC) observations at different magnetic local times (MLTs). The three panels (from top to bottom) represent 19, 22, and 0 MLTs. The left panels show AMPERE FAC densities in red-blue colored contours, and the right panels show GPS TEC measurements in blue contours. The black dots show the latitude of SAPS measurements obtained by the US mid-latitude Super Dual Auroral Radar Network (SuperDARN) radars.

at 22 MLT but less so at 0 MLT. The lower panels examine the relationship between the TEC trough and SAPS speeds at 22 and 0 MLTs. Typically, the formation of the trough is attributed to the decay in plasma density due to flow stagnation on the nightside where convection and corotation electric fields cancel each other (Spiro et al., 1978). In addition, increased recombination rates due to strong SAID/SAPS electric fields (Spiro et al., 1979) can further deepen the trough. During this event interval, we find that the TEC trough steadily deepens throughout the event at 22 MLT but at 0 MLT it only starts to deepen after the SAPS flows have started to decay. These observations suggest that at 22 MLT the elevated SAPS speeds during the initial phases (reaching 1000 m/s at 0450 UT) might be contributing to the deepening of the trough. On the other hand, at 0 MLT, it is likely that flow stagnation is predominantly determining the trough dynamics, and SAPS flows may not have a significant impact in deepening the TEC trough.

4. Discussion

In the previous sections, we presented measurements of SAPS flows observed by the US mid-latitude SuperDARN radars during the recovery phase of a minor geomagnetic storm on July 5, 2011. We examined the variability in SAPS speed and location compared with the magnitude and location of the FACs and the TEC trough. In this section, we discuss the extent to which these observations are consistent with prevailing theories for SAPS formation.

Current paradigms for SAPS formation rely on current closure across the low-conducting mid-latitude ionospheric trough (P. C. Anderson et al., 1993; Banks & Yasuhara, 1978; Schunk et al., 1976), either between the Region-2 and Region-1 currents (Foster & Burke, 2002, and references therein), or between inner and outer loops of the substorm current wedge (Mishin et al., 2017). Both scenarios place the majority of SAPS flows between two MLT-extended FAC sheets with an upward current poleward of a downward current corresponding to a poleward electric field. If such current closure is a dominant influence then the speed of the SAPS flows should depend on the strength of the FACs and, in some cases, the depth of the trough as well. However, this event presents several inconsistencies with these expectations.

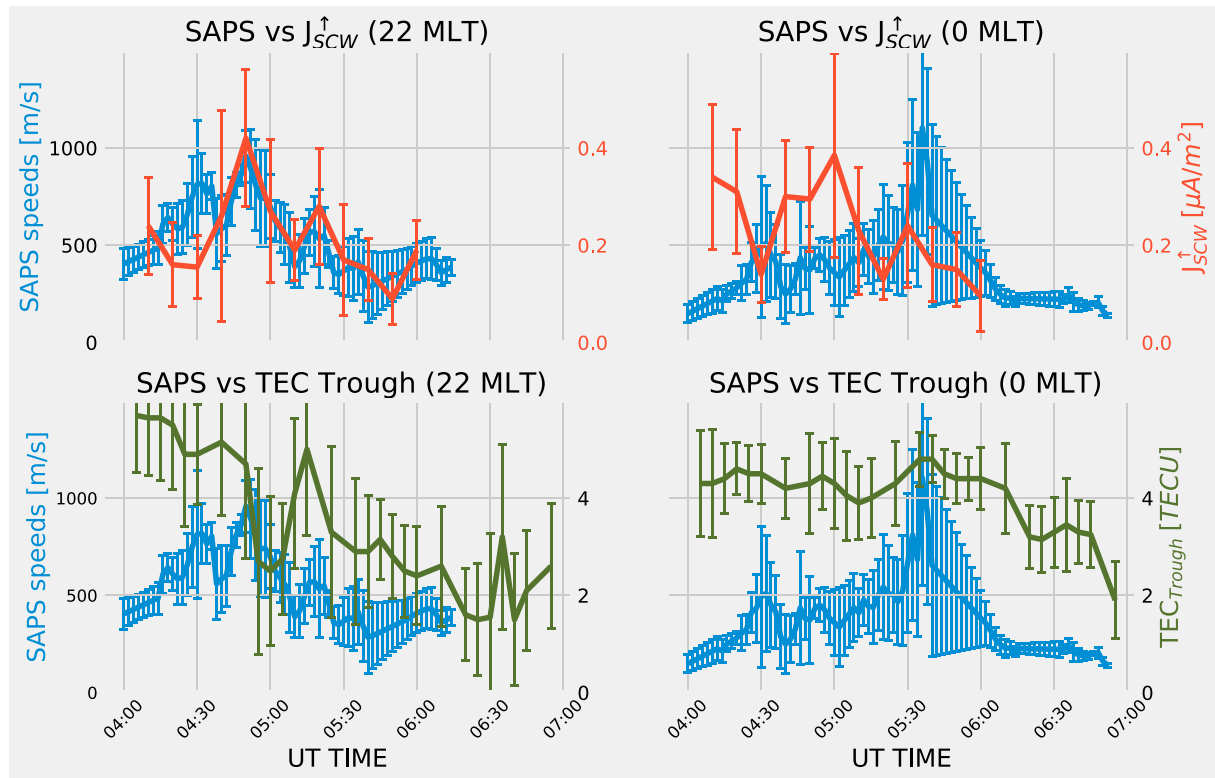


Figure 4. Time series plots comparing the magnitude of 2-D sub-auroral polarization stream velocity vectors (see text for details) with J_{SCW}^{\uparrow} (top panels), and depth of the mid-latitude trough (bottom panels) at 22 (left) and 0 (right) magnetic local times. The solid lines indicate median values and the error bars represent the corresponding standard deviations.

First, most of the SAPS flows observed by the SuperDARN radars are not sandwiched between upward and downward FACs but equatorward of all prominent FACs identified by AMPERE (Figures 2 and 3). If ionospheric closure of FACs is driving the SAPS flows then there must be additional weaker FACs even more equatorward with current densities below the $0.16 \mu A/m^2$ threshold of AMPERE (B. J. Anderson et al., 2014). This scenario is possible, but horizontal closure of ionospheric currents produced by storm-time ionosphere-thermosphere processes, such as the ionospheric disturbance dynamo (Blanc & Richmond, 1980), is also likely. However, it is important to note that the disturbance dynamo mechanism is typically expected to have a response time of several hours (Blanc & Richmond, 1980), which is longer than the timescales reported in this event. Finally, the magnetospheric drivers controlling subauroral flows can vary depending on the phase and the strength of the storm.

Second, the location of the SAPS flows relative to upward/downward FACs and their correlation with FAC magnitude varies with local time. At 19 MLT, the SAPS flows are mostly equatorward of a downward FAC while at 22 and 0 MLT they are mostly equatorward of an upward FAC (Figures 2 and 3). At 22 MLT, the SAPS speed is somewhat correlated with the intensity of the upward FAC and the TEC trough decreases throughout the event (Figure 4), consistent with expectations for FAC closure. However, at 0 MLT, the SAPS speed and FAC intensity are anti-correlated, the SAPS flows persist for some time after the upward FAC has retreated poleward and essentially disappeared, and the TEC trough only starts to decrease after the SAPS flows have decayed (Figure 4). Reconciling these vastly different behaviors at different MLTs with a common magnetospheric driver via ionospheric closure of FACs, is difficult, to say the least.

The one feature of this event that is consistent with the traditional FAC closure paradigm across all local times is that the SAPS flows were firmly embedded inside the trough throughout the event, even after the FACs retreated poleward and weakened substantially. This suggests ionosphere-thermosphere processes occurring in the vicinity of the trough may play a much more important role than previously realized

in controlling SAPS dynamics and sustaining the SAPS flows after the initial magnetospheric driver has weakened.

5. Conclusions

In this study, we presented SuperDARN observations of SAPS during the recovery phase of a minor geomagnetic storm and examined the location and strength of the flows in relation to the large-scale configuration of AMPERE FACs and the GPS TEC trough. The SAPS flows developed when a resurgence of substorm activity drove a new set of FACs into the ionosphere but the relation between upward/downward FACs to SAPS varied with MLT and most of the SAPS flows were equatorward of the strongest FACs. During the declining phase of the event, the FACs weakened in magnitude and retreated poleward while the SAPS flows weakened but remained fixed inside the trough and persisted much longer near the midnight sector than at earlier MLTs. Taken together, these observations are inconsistent with the traditional paradigm that SAPS flows are produced by ionospheric closure between parallel sheets of upward and downward FACs. Across all MLTs, the SAPS flows remained firmly embedded in the trough, suggesting that thermosphere-ionosphere processes occurring inside the trough play an important role in specifying the SAPS latitude and sustaining the flows even after the magnetospheric driver has weakened.

Data Availability Statement

SuperDARN data used in this study can be obtained from the Virginia Tech SuperDARN group (<http://vt.superdarn.org/tiki-index.php>). The Iridium-derived AMPERE data used in this paper can be obtained from the AMPERE Science Center (at <http://ampere.jhuapl.edu/>). GPS TEC data used in this study can be obtained by selecting the “World-wide GNSS Receiver Network (1998–2021)” from the instruments section on <http://www.openmadrigal.org>. Data for TEC processing are provided from the following organizations: UNAVCO, Scripps Orbit and Permanent Array Center, Institut Geographique National, France, International GNSS Service, The Crustal Dynamics Data Information System (CDDIS), National Geodetic Survey, Instituto Brasileiro de Geografia e Estatística, RAMSAC CORS of Instituto Geográfico Nacional de la República Argentina, Arecibo Observatory, Low-Latitude Ionospheric Sensor Network (LISN), Topcon Positioning Systems, Inc., Canadian High Arctic Ionospheric Network, Centro di Ricerche Sismologiche, Système d’Observation du Niveau des Eaux Littorales (SONEL), RENAG: REseau NATIONAL GPS permanent, GeoNet—the official source of geological hazard information for New Zealand, GNSS Reference Networks, Finnish Meteorological Institute, and SWEPOS—Sweden. Access to these data are provided by madrigal network via: <http://cedar.openmadrigal.org/>. The OMNI data used in this paper can be obtained from NASA/GSFC’s Space Physics Data Facility’s CDAweb service (at <http://cdaweb.gsfc.nasa.gov/>) and selecting the “OMNI (Combined 1 AU IP Data; Magnetic and Solar Indices)” option. DMSP data used in the supplementary analysis can be obtained from: https://w3id.org/cedar?experiment_list=experiments3/2011/dms/05jul11&file_list=dms_20110705_18e.001.hdf5 and https://w3id.org/cedar?experiment_list=experiments3/2011/dms/05jul11&file_list=dms_20110705_18s1.001.hdf5. A description of DMSP magnetometer data can be found in Kilcommons et al. (2017). The majority of analysis and visualization were completed with the help of free, open-source software tools such as matplotlib (Hunter, 2007), IPython (Pérez & Granger, 2007) and pandas (McKinney, 2010).

Acknowledgments

The authors thank the National Science Foundation for support under grants AGS-1822056, AGS-1839509, and AGS-1935110. The authors acknowledge the use of SuperDARN data. SuperDARN is a collection of radars funded by national scientific funding agencies of Australia, Canada, China, France, Italy, Japan, Norway, South Africa, United Kingdom and the United States of America. TEC data is provided to the community by the Massachusetts Institute of Technology (MIT) under support from US National Science Foundation grant AGS-1952737.

References

- Anderson, B. J., Korth, H., Waters, C. L., Green, D. L., Merkin, V. G., Barnes, R. J., & Dyrd, L. P. (2014). Development of large-scale birkeland currents determined from the active magnetosphere and planetary electrodynamics response experiment. *Geophysical Research Letters*, 41(9), 3017–3025. <https://doi.org/10.1002/2014GL059941>
- Anderson, B. J., Takahashi, K., & Toth, B. A. (2000). Sensing global Birkeland currents with iridium® engineering magnetometer data. *Geophysical Research Letters*, 27(24), 4045–4048. <https://doi.org/10.1029/2000GL000094>
- Anderson, P. C., Carpenter, D. L., Tsuruda, K., Mukai, T., & Rich, F. J. (2001). Multisatellite observations of rapid subauroral ion drifts (SAID). *Journal of Geophysical Research*, 106(A12), 29585–29599. <https://doi.org/10.1029/2001JA000128>
- Anderson, P. C., Hanson, W. B., Heelis, R. A., Craven, J. D., Baker, D. N., & Frank, L. A. (1993). A proposed production model of rapid subauroral ion drifts and their relationship to substorm evolution. *Journal of Geophysical Research*, 98(A4), 6069–6078. <https://doi.org/10.1029/92JA01975>
- Banks, P. M., & Yasuhara, F. (1978). Electric fields and conductivity in the nighttime E-region: A new magnetosphere-ionosphere-atmosphere coupling effect. *Geophysical Research Letters*, 5(12), 1047–1050. <https://doi.org/10.1029/GL005i012p01047>

- Birn, J., & Hesse, M. (2013). The substorm current wedge in MHD simulations. *Journal of Geophysical Research: Space Physics*, 118(6), 3364–3376. <https://doi.org/10.1002/jgra.50187>
- Blanc, M., & Richmond, A. (1980). The ionospheric disturbance dynamo. *Journal of Geophysical Research*, 85(A4), 1669–1686. <https://doi.org/10.1029/JA085iA04p01669>
- Chisham, G., Lester, M., Milan, S. E., Freeman, M. P., Bristow, W. A., Grocott, A., et al. (2007). A decade of the super dual auroral radar network (SuperDARN): Scientific achievements, new techniques and future directions. *Surveys in Geophysics*, 28(1), 33–109. <https://doi.org/10.1007/s10712-007-9017-8>
- Davis, T. N., & Sugiura, M. (1966). Auroral electrojet activity index ae and its universal time variations. *Journal of Geophysical Research*, 71(3), 785–801. <https://doi.org/10.1029/JZ071i003p00785>
- Erickson, P. J., Beroz, F., & Miskin, M. Z. (2011). Statistical characterization of the American sector subauroral polarization stream using incoherent scatter radar. *Journal of Geophysical Research*, 116(A5), A00J21. <https://doi.org/10.1029/2010JA015738>
- Ferdousi, B., Nishimura, Y., Maruyama, N., & Lyons, L. R. (2019). Subauroral neutral wind driving and its feedback to saps during the 17 march 2013 geomagnetic storm. *Journal of Geophysical Research: Space Physics*, 124(3), 2323–2337. <https://doi.org/10.1029/2018JA026193>
- Foster, J. C., & Burke, W. J. (2002). SAPS: A new categorization for sub-auroral electric fields. *Eos, Transactions American Geophysical Union*, 83(36), 393–394. <https://doi.org/10.1029/2002EO000289>
- Gussenhoven, M. S., Hardy, D. A., & Heinemann, N. (1987). The equatorward boundary of auroral ion precipitation. *Journal of Geophysical Research*, 92(A4), 3273–3283. <https://doi.org/10.1029/JA092iA04p03273>
- He, F., Zhang, X., Wang, W., Liu, L., Ren, Z., Yue, X., et al. (2018). Large-scale structure of subauroral polarization streams during the main phase of a severe geomagnetic storm. *Journal of Geophysical Research*, 123(4), 2964–2973. <https://doi.org/10.1002/2018JA025234>
- Heinemann, N. C., Gussenhoven, M. S., Hardy, D. A., Rich, F. J., & Yeh, H.-C. (1989). Electron/ion precipitation differences in relation to region 2 field-aligned currents. *Journal of Geophysical Research*, 94(A10), 13593–13600. <https://doi.org/10.1029/JA094iA10p13593>
- Hunter, J. D. (2007). Matplotlib: A 2D graphics environment. *Computing in Science & Engineering*, 9(3), 90–95. <https://doi.org/10.1109/MCSE.2007.55>
- Iyemori, T. (1990). Storm-time magnetospheric currents inferred from mid-latitude geomagnetic field variations. *Journal of Geomagnetism and Geoelectricity*, 42(11), 1249–1265. <https://doi.org/10.5636/jgg.42.1249>
- Kepko, L., McPherron, R. L., Amm, O., Apatenkov, S., Baumjohann, W., Birn, J., et al. (2015). Substorm current wedge revisited. *Space Science Reviews*, 190(1), 1–46. <https://doi.org/10.1007/s11214-014-0124-9>
- Kilcommons, L. M., Redmon, R. J., & Knipp, D. J. (2017). A new DMSP magnetometer and auroral boundary data set and estimates of field-aligned currents in dynamic auroral boundary coordinates. *Journal of Geophysical Research: Space Physics*, 122(8), 9068–9079. <https://doi.org/10.1002/2016JA023342>
- King, J. H., & Papitashvili, N. E. (2005). Solar wind spatial scales in and comparisons of hourly wind and ace plasma and magnetic field data. *Journal of Geophysical Research*, 110(A2). <https://doi.org/10.1029/2004JA010649>
- Kunduri, B. S. R., Baker, J. B. H., Ruohoniemi, J. M., Nishitani, N., Oksavik, K., Erickson, P. J., et al. (2018). A new empirical model of the sub-auroral polarization stream. *Journal of Geophysical Research: Space Physics*, 123(9), 7342–7357. <https://doi.org/10.1029/2018JA025690>
- Kunduri, B. S. R., Baker, J. B. H., Ruohoniemi, J. M., Thomas, E. G., Shepherd, S. G., & Sterne, K. T. (2017). Statistical characterization of the large-scale structure of the sub-auroral polarization stream. *Journal of Geophysical Research*, 122(6). <https://doi.org/10.1002/2017JA024131>
- Lejosne, S., Kunduri, B. S. R., Mozer, F. S., & Turner, D. L. (2018). Energetic electron injections deep into the inner magnetosphere: A result of the subauroral polarization stream (SAPS) potential drop. *Geophysical Research Letters*, 45, 3811–3819. <https://doi.org/10.1029/2018GL077969>
- Makarevich, R. A., Kellerman, A. C., Devlin, J. C., Ye, H., Lyons, L. R., & Nishimura, Y. (2011). Saps intensification during substorm recovery: A multi-instrument case study. *Journal of Geophysical Research*, 116(A11). <https://doi.org/10.1029/2011JA016916>
- McKinney, W. (2010). Data structures for statistical computing in python. In van der Walt, S., & Millman, J. (Eds.), *Proceedings of the 9th python in science conference* (pp. 51–56). SciPy Conference. <https://doi.org/10.25080/majora-92b1f1922-00a>
- Mishin, E. (2016). Saps onset timing during substorms and the westward traveling surge. *Geophysical Research Letters*, 43(13), 6687–6693. <https://doi.org/10.1002/2016GL069693>
- Mishin, E., Nishimura, Y., & Foster, J. (2017). Saps/said revisited: A causal relation to the substorm current wedge. *Journal of Geophysical Research*, 122(8), 8516–8535. <https://doi.org/10.1002/2017JA024263>
- Murphy, K. R., Mann, I. R., Rae, I. J., Waters, C. L., Frey, H. U., Kale, A., et al. (2013). The detailed spatial structure of field-aligned currents comprising the substorm current wedge. *Journal of Geophysical Research*, 118(12), 7714–7727. <https://doi.org/10.1002/2013JA018979>
- Nishitani, N., Ruohoniemi, J. M., Lester, M., Baker, J. B. H., Koustov, A. V., Shepherd, S. G., et al. (2019). Review of the accomplishments of mid-latitude super dual auroral radar network (SuperDARN) HF radars. *Progress in Earth and Planetary Science*, 6(1), 1–57. <https://doi.org/10.1186/s40645-019-0270-5>
- Parkinson, M. L., Pinnock, M., Ye, H., Hairston, M. R., Devlin, J. C., Dyson, P. L., et al. (2003). On the lifetime and extent of an auroral westward flow channel (AWFC) observed during a magnetospheric substorm. *Annales Geophysicae*, 21(4), 893–913. <https://doi.org/10.5194/angeo-21-893-2003>
- Pérez, F., & Granger, B. E. (2007). IPython: A system for interactive scientific computing. *Computing in Science & Engineering*, 9(3), 21–29. <https://doi.org/10.1109/MCSE.2007.53>
- Rideout, W., & Coster, A. (2006). Automated GPS processing for global total electron content data. *GPS Solutions*, 10(3), 219–228. <https://doi.org/10.1007/s10291-006-0029-5>
- Ruohoniemi, J. M., Greenwald, R. A., Baker, K. B., Villain, J. P., & McCready, M. A. (1987). Drift motions of small-scale irregularities in the high-latitude F region: An experimental comparison with plasma drift motions. *Journal of Geophysical Research*, 92(A5), 4553–4564. <https://doi.org/10.1029/JA092iA05p04553>
- Sangha, H., Milan, S. E., Carter, J. A., Fogg, A. R., Anderson, B. J., Korth, H., & Paxton, L. J. (2020). Bifurcated region 2 field-aligned currents associated with substorms. *Journal of Geophysical Research: Space Physics*, 125(1), e2019JA027041. <https://doi.org/10.1029/2019JA027041>
- Schunk, R. W., Banks, P. M., & Raitt, W. J. (1976). Effects of electric fields and other processes upon the nighttime high-latitude F layer. *Journal of Geophysical Research*, 81(19), 3271–3282. <https://doi.org/10.1029/JA081i019p03271>
- Shepherd, S. G. (2014). Altitude-adjusted corrected geomagnetic coordinates: Definition and functional approximations. *Journal of Geophysical Research: Space Physics*, 119(9), 7501–7521. <https://doi.org/10.1002/2014JA020264>
- Spiro, R. W., Heelis, R. A., & Hanson, W. B. (1978). Ion convection and the formation of the mid-latitude F region ionization trough. *Journal of Geophysical Research*, 83(A9), 4255–4264. <https://doi.org/10.1029/JA083iA09p04255>

- Spiro, R. W., Heelis, R. A., & Hanson, W. B. (1979). Rapid subauroral ion drifts observed by atmosphere explorer C. *Geophysical Research Letters*, 6(8), 657–660. <https://doi.org/10.1029/GL006i008p00657>
- Thomas, E. G., Baker, J. B. H., Ruohoniemi, J. M., Clausen, L. B. N., Coster, A. J., Foster, J. C., & Erickson, P. J. (2013). Direct observations of the role of convection electric field in the formation of a polar tongue of ionization from storm enhanced density. *Journal of Geophysical Research*, 118(3), 1180–1189. <https://doi.org/10.1002/jgra.50116>
- Vierinen, J., Coster, A. J., Rideout, W. C., Erickson, P. J., & Norberg, J. (2016). Statistical framework for estimating GNSS bias. *Atmospheric Measurement Techniques*, 9(3), 1303–1312. <https://doi.org/10.5194/amt-9-1303-2016>
- Waters, C. L., Anderson, B. J., & Liou, K. (2001). Estimation of global field aligned currents using the iridium® system magnetometer data. *Geophysical Research Letters*, 28(11), 2165–2168. <https://doi.org/10.1029/2000GL012725>